Published in final edited form as:
Bioconjug Chem. 2009 September 14; 20(10): 1853–1859. doi:10.1021/bc900217h.

RGD Dendron bodies; synthetic avidity agents with defined and potentially interchangeable effector sites that can substitute for antibodies

Daniel Q. McNerny[†,‖], **Jolanta F. Kukowska-Latallo**[†], **Douglas G. Mullen**[†,‡], **Joseph M. Wallace**[†,§], **Ankur M. Desai**[†], **Rameshwer Shukla**[†], **Baohua Huang**[†], **Mark M. Banaszak Holl**[†,‡,§], and **James R. Baker Jr.**[*,†,^]
Michigan Nanotechnology Institute for Medicine and Biological Sciences, Department of Chemical Engineering, Program in Macromolecular Science and Engineering, Department of Chemistry, Department of Internal Medicine, University of Michigan, Ann Arbor, MI 48109

Abstract

Poly(amidoamine) (PAMAM) dendrons were synthesized with c(RGDyK) peptide on the surface to create a scaffold for cellular targeting and multivalent binding. Binary dendron-RGD conjugates were synthesized with a single Alexa Fluor 488, biotin, methotrexate drug molecule, or additional functionalized dendron at the focal point. The targeted-dendron platform was shown to specifically target $\alpha_V\beta_3$ integrin expressing human umbilical vein endothelial cells (HUVEC) and human glioblastoma cells (U87MG) *in vitro* via flow cytometry. Specific targeting of the dendron-RGD platform was further confirmed by confocal microscopy. Biological activity of the targeted drug conjugate was confirmed via XTT assay. The orthogonal reaction chemistry used at thedendron focal point gives a precise 1:1 ratio of the attachment of multiple functionalities to a small molecular weight, chemically stable high avidity molecule. These studies serve as a framework to selectively combine biologically relevant functions with enhanced specific binding activity to substitute for antibodies in many diagnostic and therapeutic applications.

INTRODUCTION

The development of specific targeting molecules for diagnostic and therapeutic applications is an important goal being pursued by the biomedical community. Precise targeting of molecules, cellular compartments or tissues has the potential to positively affect a broad range of disciplines including diagnostic and imaging technologies, and could enhance the treatment of a wide range of conditions such as inflammation, infectious diseases, and cancer. The most common molecules currently employed for numerous applications are monoclonal antibodies (1,2), or immunoconjugates of these antibodies, which take advantage of their high specific binding affinities for antigens. Almost all specific

[*]Corresponding author. jbakerjr@med.umich.edu, Michigan Nanotechnology Institute for Medicine and Biological Sciences, 9220 MSRB III, Box 5648, University of Michigan, Ann Arbor, MI 48109.
[†]Michigan Nanotechnology Institute for Medicine and Biological Sciences, University of Michigan
[‖]Department of Chemical Engineering, University of Michigan
[‡]Program in Macromolecular Science and Engineering, University of Michigan.
[§]Department of Chemistry, University of Michigan
[^]Department of Internal Medicine, University of Michigan

Supporting Information Available: ^{1}H NMR and UPLC/HPLC characterization of dendron conjugates. This material is available free of charge via the Internet at http://pubs.acs.org/BC.

diagnostics are now based on some form of immunoconjugate (3–7), and numerous monoclonal antibody-based therapeutics are FDA-approved to meet clinical needs (8,9).

Despite these successes, immunoconjugates suffer from significant disadvantages. There are many small molecules that are not immunogenic, and therefore cannot be identified by antibodies. In addition, antibodies are proteins that denature under many chemical and thermal conditions, and therefore necessitate strict refrigeration requirements for diagnostic kits or therapeutics based on immunoconjugates. The large size (approximately 150 kDa) of immunoconjugates limits blood clearance and potentially causes slow tumor penetration (10,11). Being foreign proteins, antibodies elicit immunogenic responses in patients that limit their therapeutic utility (12,13). Finally, biological molecules are difficult and costly to produce in bulk (14). Thus, alternative molecules to antibodies are needed.

Poly(amidoamine) (PAMAM) dendritic macromolecules are controllable in size and have defined, monodisperse (PDI = 1.02) structures. The macromolecule is significantly smaller than antibodies, which allows the device to enter the cell to potentially treat multiple proliferation pathways. In addition, the polyamide backbone helps the macromolecule maintain water solubility and minimizes immunogenicity (15,16). The dendritic macromolecules also have large numbers of surface primary amines created by a branched architecture that allow for the attachment of multiple molecules with various functions. This has been demonstrated with targeting ligands, imaging agents and therapeutics (17,18). The ability to conjugate multiple targeting moieties provides the opportunity to create a platform with increased binding avidity through polyvalent cell interactions (19). Targeted dendrimer delivery platforms have been successfully tested in *in vitro* and *in vivo* model tumor systems (20–29).

To increase the utility of the dendritic scaffold, orthogonal and modular pathways can be used to construct binary devices with a greater degree of specificity and flexibility. However, current research pursuing such pathways to create functional dendritic devices has been sparse. PAMAM dendrimers have been developed with unique surface groups for modular synthesis via click chemistry (30), complimentary oligonucleotide hybridization (31), or orthogonal functionalization (32). Dendrons with a bis-MPA backbone have been utilized by exploiting the unique reactive site at the focal point to create bi-functional materials (33). These approaches offer the potential to construct individual combinations for a specific targeting application from a common library of functionalized devices in a versatile manner and overcome the inefficiencies of step-wise conjugations on a single dendritic macromolecule. However, the central advantage of these techniques is that they provide increased homogeneity products by reducing the complexity of ligand distributions created by multi-functional platforms.

Herein, we present the synthesis and evaluation of *in vitro* biological activity for a targeted, PAMAM dendron avidity platform (Figure 1). The functionalized PAMAM dendron can maintain the binding specificity and multivalency of previous dendritic models (25,34) while creating an orthogonally coupled scaffold more suitable for personalized medicine and applications. Binary devices were synthesized through a unique alkyne group at the dendron focal point. The alkyne is reacted with an azide-functionalized dye, biotin, therapeutic molecule or a second dye-conjugated dendron in a copper-catalyzed 1,3-dipolar cycloaddition, commonly referred to as “click chemistry” (35). This strategy is attractive because it provides high versatility and yields, mild reaction conditions and no alteration to neighboring functional groups that eliminates the need for protecting groups. The platform itself gives a precise 1:1 ratio of the attachment of multiple functionalities, preventing aggregate formation. A dendron with multiple Arg-Gly-Asp (RGD) adhesion ligands on the surface and an additional function at the focal point can specifically target $\alpha_V\beta_3$ integrin

expressing human umbilical vein endothelial cells (HUVEC) and human glioblastoma cells (U87MG), displaying the biological utility of the platform. The dendron-RGD platform also successfully inhibits tumor growth when conjugated to a therapeutic drug, such as methotrexate (MTX). Thus, the ability to conjugate specific and varied effector sites to the dendron periphery to generate a high avidity binding agent and use orthogonal reaction chemistry at the focal point to add additional functionalities makes these "dendro–bodies" an attractive alternative to antibodies for targeting applications.

EXPERIMENTAL PROCEDURES

General

Alexa Fluor 488 azide and Prolong Gold mounting agent were obtained from Invitrogen. c(RGDyK) peptide was obtained from Peptide International. Biotin-dPEG$_{3+4}$-azide was obtained from Quanta Biodesign. Sephadex G15 and G25 were obtained from GE Life Sciences. Spectra/Por 7 dialysis membrane (MWCO 1000) was obtained from Spectrum Laboratories. NeutrAvidin-Dylight 405 was obtained from Pierce. All other chemicals were obtained from Sigma. All purified reaction products were characterized by ^{1}H NMR, HPLC, and matrix-assisted laser desorption-ionization time-of-flight (MALDI-TOF) mass spectrometry.

Synthesis of alkyne-G3-PAMAM. dendron (1)

Alkyne-G3-PAMAM dendron was prepared as previously reported (36) and analyzed by ^{1}H and ^{13}C NMR and MALDI-TOF. MS (MALDI): 3479 Da; calculated for $C_{153}H_{305}N_{61}O_{30}$: 3479.45 Da.

Synthesis of alkyne-G3(COOH)$_{16}$ (2)

Glutaric anhydride (0.0164 g, 0.1437 mmol) dissolved in anhydrous MeOH (0.8 mL) was added dropwise to a solution of **1** (0.0200 g, 0.0057 mmol) and triethylamine (Et_3N) (0.0186 g, 0.1838 mol) in anhydrous MeOH (0.2 mL) while stirring, and the reaction mixture was allowed to stir for 24 hours at room temperature. All solvent was removed in vacuo, and the reaction material was dissolved in H_2O, purified on a G-15 Sephadex column and lyophilized. MS (MALDI): 5305 Da; calculated for $C_{233}H_{401}N_{61}O_{78}$: 5305.04 Da.

Synthesis of alkyne-G3(COOH)$_{11.9}$(RGD)$_{4.1}$ (3)

1-(3-(dimethylamino)propyl)-3- ethylcarbodiimide HCl (EDC) (0.0838 g, 0.4373 mmol) was allowed to react with **2** (0.0145 g, 0.0027 mmol) in 1:1 H_2O/DMSO (2 mL) for 2 hours to form an active ester. c(RGDyK) (0.0169 g, 0.0273 mmol) in 4:1 H_2O/DMSO (1.25mL) was added dropwise to the EDC and dendron solution and stirred for 2 days at room temperature. The DMSO was removed via dialysis in H_2O for 1 hour. The resulting solution was lyophilized, redissolved in H_2O, and purified on a G-15 Sephadex column, then again lyophilized. MS (MALDI): 5300–12000 Da (broad).

Synthesis of AF-G3(COOH)$_{11.9}$(RGD)$_{4.1}$ (4)

A mixture of azide-functionalized Alexa Fluor 488 (0.00022 g, 0.0002 mmol) and **3** (0.0015 g, 0.0002 mmol) in H_2O (1 mL) in the presence of copper(II) sulfate (2.5×10^{-5} g, 0.0001 mmol) and sodium ascorbate (4.0×10^{-5} g, 0.0002 mmol) was stirred for 36 hours at room temperature. The solution was purified on a G-25 Sephadex column and lyophilized. MS (MALDI): 5300–12600 Da (broad).

Synthesis of MTX-azide (5)

Methotrexate (0.0238 g, 0.05237 mmol) was dissolved in DMF (1 mL) and cooled in a water/ice bath. *N*-Hydroxysuccinimide (0.0067 g, 0.0576 mmol) and EDC (0.0110 g, 0.0576 mmol) were added, and the resulting mixture was stirred in the ice bath for 30 min to give a white precipitate. A solution of 11-azido-3,6,9- trioxaundecan-1-amine (0.0120 g, 0.0550 mmol) in DMF (0.5 mL) was added, and the resulting mixture was allowed to warm to room temperature and stirred for 24 h. The mixture was poured into water (50 mL) and washed with chloroform (50 mL × 3). The aqueous layer was lyophilized and further purified on a G-25 Sephadex column. MS: 654.7 Da; calculated for $C_{28}H_{38}N_{12}O_7$: 654.68 Da.

Synthesis of MTX-G3(COOH)$_{11.9}$(RGD)$_{4.1}$ (6)

A mixture of **5** (0.0019 g, 0.0029 mmol) and **3** (0.0025 g, 0.0003 mmol) in H_2O (1 mL) in the presence of copper(II) sulfate (2.5×10^{-5} g, 0.0001 mmol) and sodium ascorbate (4.0×10^{-5} g, 0.0002 mmol) was stirred for 36 hours at room temperature. The solution was purified on a G-25 Sephadex column and lyophilized. MS (MALDI): 5300–12600 Da (broad).

Synthesis of biotin-G3(COOH)$_{11.9}$(RGD)$_{4.1}$ (7)

A mixture of biotin-dPEG$_{3+4}$-azide (0.0045 g, 0.0006 mmol) and **3** (0.0080 g, 0.0001 mmol) in 1:1 DMSO/H_2O (1 mL) in the presence of copper(II) sulfate (2.5×10^5 g, 0.0001 mmol) and sodium ascorbate (4.0×10^5 g, 0.0002 mmol) was stirred for 36 hours at room temperature. The solution was purified on a G-25 Sephadex column and lyophilized. MS (MALDI): 5300–12700 Da (broad).

Synthesis of azide-G2-PAMAM dendron (8)

Azide-G2-PAMAM dendron was prepared as previously reported (37) and analyzed by ^1H and MALDI-TOF. MS (MALDI): 1698.1 Da; calculated for $C_{73}H_{148}N_{32}O_{14}$: 1698.16 Da.

Synthesisof azide-G2(AF)$_2$(OH)$_{24}$ (9)

Alexa Fluor 488 sulfodichlorophenol ester (0.0050 g, 0.0061 mmol) dissolved in 0.5 mL DMF was added dropwise to **8** (0.0028 g, 0.0015 mmol) in 0.5 mL 0.1 M sodium bicarbonate buffer while stirring, and the reaction mixture was allowed to stir for 24 hours at room temperature. Solvent was removed in vacuo, and the resulting product was dissolved in 2 mL H_2O. Glycidol (0.0112 g, 0.1506 mmol) was added to the solution and the mixture was allowed to stir for 24 hours at room temperature. The solution was purified on a G-25 Sephadex column and lyophilized. MS (MALDI): 3000–7000 Da (broad).

Synthesis of (OH)$_{24}$(AF)$_2$G2-G3(COOH)$_{11.9}$(RGD)$_{4.1}$ co-dendron (10)

A mixture of **9** (0.0030 g, 0.0009 mmol) and **3** (0.0044 g, 0.0006 mmol) in H_2O (1 mL) in the presence of copper(II) sulfate (2.5×10^5 g, 0.0001 mmol) and sodium ascorbate (4.0×10^5 g, 0.0002 mmol) was stirred for 36 hours at room temperature. The solution was first purified on a G-25 Sephadex column and lyophilized. The product was further purified via HPLC to remove excess azide-G2(AF)(OH). MS (MALDI): 5000–29000 Da (broad), 17500 Da maximum.

Cell Culture and incubation with the dendron

HUVEC cells were obtained from Invitrogen (Cascade Biologics). U87MG and KB cells were obtained from American Type Tissue Collection (Manasass, VA). HUVEC cells (cat. # C-015–10C), U87MG and KB cells were grown and maintained according to the supplier's protocol. Compounds were prepared in non-supplemented cell culture medium (Medium

200) and incubated in cell suspensions for 2 hours at 37 °C in a 5% CO_2 incubator. Blocking experiments were run by pre-incubating the cells with a 200 equivalent excess of c(RGDyK) for 10 minutes at room temperature prior to incubation.

Flow Cytometry

Cells were washed with 5mL of PBS, spun at 150 G for 7 minutes, and re-suspended in 1 mL of PBS prior to being examined. Cells were examined quantitatively for dendron uptake via a flow cytometer (Beckman Coulter Epics XL-MCL). The FL1 fluorescence of 10000 cells was measured and the mean fluorescence of cells was quantified.

Confocal Microscopy

HUVEC cells were seeded and grown on 35 mm glass-bottomed culture dishes (MatTek Corp., Ashland, MA). After 2 days, cells were treated with 0.5 μM co-dendron **10** or biotin-conjugated dendron **7**. Blocked samples were run by pre-incubating the cells with a 200 equivalent excess of c(RGDyK) for 10 minutes at room temperature prior to incubation. After the 2 hour incubation period, biotin-conjugated dendron **7** treated cells were treated with 4 mg/mL BSA for 30 minutes to limit non-specific binding followed by treatment with 0.5 μM NeutrAvidin-Dylight 405 for 30 minutes. Media was aspirated from the cells, washed 3 times with PBS, and fixed with 2% paraformaldehyde. The samples were again aspirated, washed 3 times, and aspirated before mounting with Prolong Gold and a cover slip was added. Samples were imaged using an Olympus FluoView 500 Laser Scanning confocal microscope using 60X, 1.5 NA oil immersion objective. Fluorescence and differential interference contrast (DIC) images were collected simultaneously using either an argon laser with 488 nm excitation or a solid state diode laser with 405 nm excitation and *FluoView* software.

Cytotoxicity Assay

For cytotoxicity experiments, cells were seeded in 96-well microtiter plates (2500 cells/well) in Medium 200. The cells were treated in triplicate with different concentrations of free MTX or dendron conjugates for 72 hours with a replenishing of 100 μL medium and the conjugates after 48 hours. A colorimetric XTT assay (Invitrogen) was performed following the vendor's protocol. An aliquot of 30 μL of XTT working solution prepared according to manufacturer instructions was added to each well using a multichannel pipette followed by the addition of 20 μL of PBS. After 1 hour incubation in the dark at 37 °C, the absorbance at 490 nm was recorded using a plate reader. 690 nm was selected as a reference wavelength. Cell viability was calculated based on optical density (OD) from untreated cells. Statistical significance was assessed using Two-Way ANOVA with posthoc Bonferroni tests checking for main effects of conjugate and concentration. P-values less than 0.05 were considered significant.

RESULTS AND DISCUSSION

The surface amines of the G3 PAMAM dendron **1** were allowed to react with excess glutaric anhydride in MeOH, in the presence of Et_3N as base, to form carboxylic acids (Figure 2i). The reaction yielded carboxyl terminal groups and eliminates potential nonspecific charge interactions with the cell plasma membrane caused by primary amines. ^{1}H NMR spectroscopy confirmed complete conversion of the primary amines and formation of dendron **2** by the loss of methylene peaks ($–CH_2CH_2NH_2$) at δ 2.80 and 3.30 ppm and the formation of new methylene peaks ($-NHCO(CH_2)_3COOH$) at δ 1.84, 2.21, and 2.27 ppm.

The targeting moiety, RGD peptide, was conjugated to the carboxylated surface of the PAMAM dendron (Figure 2ii). RGD binds to the $\alpha_V\beta_3$ integrin found on the luminal surface

of endothelial cells during angiogenesis (38, 39). This makes the $\alpha_V\beta_3$ integrin a unique marker that differentiates newly formed capillaries in the tumor vasculature from their mature counterparts (40–42). Antiangiogenic therapies, such as ones that employ RGD targeting, prevent neovascularization by inhibiting differentiation, migration and proliferation of endothelial cells (43).

The surface carboxyl groups were activated with EDC, followed by the addition of 12 equivalents of c(RGDyK) to give dendron **3**. The product was purified by size exclusion chromatography and lyophilized. The ^{1}H NMR spectrum of the dendron-RGD body shows some of the aliphatic signals of the peptide overlap with the aliphatic signals of the dendron; however, using the peak integration values in the aromatic region from the phenyl ring of the peptide, an average of 4.1 attached RGD per dendron was calculated.

The dendron AF-G3$(COOH)_{11.9}(RGD)_{4.1}$ **4** (Figure 2iii) was synthesized by the reaction of azide-functionalized Alexa Fluor 488 with **3** in a copper-catalyzed 1,3-dipolar cycloaddition. Alexa Fluor 488 was chosen as the fluorescent label for detection of conjugates by flow cytometry because it is brighter than fluorescein conjugates and more resistant to photobleaching. The products were purified via size exclusion chromatography and lyophilized. The characteristic triazole proton peak of a successful click reaction (δ 8.10 ppm) partially overlaps with the peaks for Alexa Fluor 488.

The specific binding of **4** to $\alpha_V\beta_3$ integrin expressing HUVEC and U87MG cells was examined via flow cytometry (Figure 3). KB cells, which express lower levels of $\alpha_V\beta_3$ integrin, were also evaluated. Cells were treated with dendron-RGD conjugates at final concentrations of 0.25, 0.50, 1, 2, and 4 μM, either with or without preincubation with 200 fold molar equivalences of free RGD peptide. Specific binding and dose dependence of dendron bodies to integrin expressing cells were evaluated after the 2 hour incubation at 37 °C. The addition of excess free peptide to inhibit the uptake of the binary dendron by HUVEC and U87MG cells significantly blocked uptake. The inability to completely inhibit binding of the dendron may be due to a higher avidity of the dendron conjugate when compared to free RGD.

A co-dendron structure, $(OH)_{24}(AF)_2$G2-G3$(COOH)_{11.9}(RGD)_{4.1}$ **10** was created by reacting an Alexa Fluor 488 conjugated dendron **9** with an azide focal point with **3**. The product was purified via HPLC to remove excess **9**. The co-dendron structure offers an increased carrying capacity for conjugates, including the Alexa Fluor 488 used in this study. NMR of **9** showed an average of 2 Alexa Fluor 488 molecules attached per dendron, thus it was expected to emit a stronger signal when conjugated to **3** compared to a single dye at the focal point.

The specific binding of co-dendron **10** to $\alpha_V\beta_3$ integrin expressing HUVEC cells was determined via flow cytometry (Figure 3D). The co-dendron treated samples see the expected increase in mean fluorescence compared to mono-dye conjugated **4**. Specific binding could be significantly blocked (Figure 4), but again the higher avidity dendron conjugate out-competed free RGD. Non-targeted control **9** showed minimal non-specific uptake.

The specific binding evaluated by flow cytometry was confirmed by confocal microscopy. HUVEC cells were treated with 0.5 μM **10** or biotin-conjugated **7** and incubated for 2 hours. The biotin-conjugate was detected by the addition of an avidin-functionalized dye. Confocal images confirm the uptake of the dendrons (Figure 5B, D), as seen from the punctuate pattern within the cytoplasm. Partial inhibition of the dendron conjugates by preincubation with free RGD was also established (Figure 5C, E).

A drug conjugate, **6** was synthesized to show the therapeutic potential of the platform. MTX was reacted with 11-azido-3,6,9-trioxaundecan-1-amine to yield an azide-functional drug. The resulting MTX-azide was then attached to the dendron at the focal point via click chemistry. The inhibition of cell growth induced by the dendron conjugates was tested by XTT colorimetric assay. **6** and free MTX showed comparable cytotoxicity to HUVEC cells after 3 days (Figure 6). Cell numbers were between 55–80% for all **6** and free MTX treated samples at concentrations greater than 0.125 μM. The effects of **6** and MTX were not significantly different at these concentrations. **6** had a significantly greater effect on cell viability versus **3** for concentrations greater than 0.125 μM. **6** has an approximately equivalent concentration of MTX compared to free drug; the drug-conjugated dendron **6** treatments may have slightly lower drug concentration due to any remaining uncoupled dendron. The similar toxicities of **6** and free MTX show that the dendron scaffold is effective at delivering a therapeutic to cells.

We have shown that by exploiting the initiation point as a unique binding site in PAMAM dendrons, selective coupling reactions can yield highly defined binary devices that exhibit the ability to bind to specific cells. Employing a 1,3-dipolar cycloaddition to the focal point of the dendron allows for additional functional moieties to be added in a precise manner without altering other molecules on the dendron. The prototype molecule, synthesized **4**, successfully displayed specific targeting to $\alpha_V\beta_3$ integrin, behaving similarly to RGD conjugates on previously studied multifunctional G5 PAMAM dendrimers (25,34) that lack the same degree of synthetic control. Detection can be enhanced by attaching an additional dendron with an increased carrying capacity, shown with **10**. The dendron can be combined with biotin, allowing it to interact with a variety of avidin-functionalized molecules. **6** was shown to successfully inhibit the growth of HUVEC cells similarly to free drug. The PAMAM dendron platform has potential to be important in targeted delivery chemistry, as our binary device can serve as a framework to selectively attach diagnostic and imaging agents, therapeutics, or other biologically relevant moieties and surfaces. In addition, coupling a second functionalized dendron or dendrimer to the dendron could address other applications requiring the delivery of multiple drugs or imaging agents.

Supplementary Material

Refer to Web version on PubMed Central for supplementary material.

Acknowledgments

This project was supported with Federal funds from the National Cancer Institute, National Institutes of Health, under award 1 R01 CA119409.

LITERATURE CITED

1. Imai K, Takaoka A. Comparing antibody and small-molecule therapies for cancer. Nat Rev Cancer 2006;6:714–727. [PubMed: 16929325]
2. Wu AM, Senter PD. Arming antibodies: Prospects and challenges for immunoconjugates. Nat Biotechnol 2005;23:1137–1146. [PubMed: 16151407]
3. Lequin RM. Enzyme immunoassay (EIA)/enzyme-linked immunosorbent assay (ELISA). Clin Chem 2005;51:2415–2418. [PubMed: 16179424]
4. Engvall E, Perlmann P. Enzyme-linked immunosorbent assay (ELISA). quantitative assay of immunoglobulin G. Immunochemistry 1971;8:871–874. [PubMed: 5135623]
5. Van Weemen BK, Schuurs AH. Immunoassay using antigen- enzyme conjugates. FEBS Lett 1971;15:232–236. [PubMed: 11945853]

6. Renart J, Reiser J, Stark GR. Transfer of proteins from gels to diazobenzyloxymethyl-paper and detection with antisera: A method for studying antibody specificity and antigen structure. Proc Natl Acad Sci USA 1979;76:3116–3120. [PubMed: 91164]
7. Towbin H, Staehelin T, Gordon J. Electrophoretic transfer of proteins from polyacrylamide gels to nitrocellulose sheets: Procedure and some applications. Proc Natl Acad Sci USA 1979;76:4350–4354. [PubMed: 388439]
8. Maloney DG, Grillo-Lopez AJ, White CA, Bodkin D, Schilder RJ, Neidhart JA, Janakiraman N, Foon KA, Liles TM, Dallaire BK, Wey K, Royston I, Davis T, Levy R. IDEC-C2B8 (rituximab) anti-CD20 monoclonal antibody therapy in patients with relapsed low-grade non-hodgkin's lymphoma. Blood 1997;90:2188–2195. [PubMed: 9310469]
9. Carter P, Presta L, Gorman CM, Ridgway JB, Henner D, Wong WL, Rowland AM, Kotts C, Carver ME, Shepard HM. Humanization of an anti-p185HER2 antibody for human cancer therapy. Proc Natl Acad Sci USA 1992;89:4285–4289. [PubMed: 1350088]
10. Carter PJ. Potent antibody therapeutics by design. Nat Rev Immunol 2006;6:343–357. [PubMed: 16622479]
11. Payne G. Progress in immunoconjugate cancer therapeutics. Cancer Cell 2003;3:207–212. [PubMed: 12676579]
12. Huang S, Armstrong EA, Benavente S, Chinnaiyan P, Harari PM. Dual-agent molecular targeting of the epidermal growth factor receptor (EGFR): Combining anti-EGFR antibody with tyrosine kinase inhibitor. Cancer Res 2004;64:5355–5362. [PubMed: 15289342]
13. Mukohara T, Engelman JA, Hanna NH, Yeap BY, Kobayashi S, Lindeman N, Halmos B, Pearlberg J, Tsuchihashi Z, Cantley LC, Tenen DG, Johnson BE, Janne PA. Differential effects of gefitinib and cetuximab on non-small-cell lung cancers bearing epidermal growth factor receptor mutations. J Natl Cancer Inst 2005;97:1185–1194. [PubMed: 16106023]
14. Weiner LM. Building better magic bullets--improving unconjugated monoclonal antibody therapy for cancer. Nat Rev Cancer 2007;7:701–706. [PubMed: 17721434]
15. Kukowska-Latallo JF, Bielinska AU, Johnson J, Spindler R, Tomalia DA, Baker JR Jr. Efficient transfer of genetic material into mammalian cells using starburst polyamidoamine dendrimers. Proc Natl Acad Sci USA 1996;93:4897–4902. [PubMed: 8643500]
16. Wiener EC, Konda S, Shadron A, Brechbiel M, Gansow O. Targeting dendrimer-chelates to tumors and tumor cells expressing the high-affinity folate receptor. Invest Radiol 1997;32:748–754. [PubMed: 9406015]
17. Majoros IJ, Thomas TP, Mehta CB, Baker JR Jr. Poly(amidoamine) dendrimer-based multifunctional engineered nanodevice for cancer therapy. J Med Chem 2005;48:5892–5899. [PubMed: 16161993]
18. Majoros IJ, Myc A, Thomas T, Mehta CB, Baker JR Jr. PAMAM dendrimer-based multifunctional conjugate for cancer therapy: Synthesis, characterization, and functionality. Biomacromolecules 2006;7:572–579. [PubMed: 16471932]
19. Hong S, Leroueil PR, Majoros IJ, Orr BG, Baker JR Jr, Banaszak Holl MM. The binding avidity of a nanoparticle-based multivalent targeted drug delivery platform. Chem Biol 2007;14:107–115. [PubMed: 17254956]
20. Kukowska-Latallo JF, Candido KA, Cao Z, Nigavekar SS, Majoros IJ, Thomas TP, Balogh LP, Khan MK, Baker JR Jr. Nanoparticle targeting of anticancer drug improves therapeutic response in animal model of human epithelial cancer. Cancer Res 2005;65:5317–5324. [PubMed: 15958579]
21. Quintana A, Raczka E, Piehler L, Lee I, Myc A, Majoros I, Patri AK, Thomas T, Mule J, Baker JR Jr. Design and function of a dendrimer- based therapeutic nanodevice targeted to tumor cells through the folate receptor. Pharm Res 2002;19:1310–1316. [PubMed: 12403067]
22. Thomas TP, Patri AK, Myc A, Myaing MT, Ye JY, Norris TB, Baker JR Jr. In vitro targeting of synthesized antibody-conjugated dendrimer nanoparticles. Biomacromolecules 2004;5:2269–2274. [PubMed: 15530041]
23. Thomas TP, Majoros IJ, Kotlyar A, Kukowska-Latallo JF, Bielinska A, Myc A, Baker JR Jr. Targeting and inhibition of cell growth by an engineered dendritic nanodevice. J Med Chem 2005;48:3729–3735. [PubMed: 15916424]

24. Wiener EC, Brechbiel MW, Brothers H, Magin RL, Gansow OA, Tomalia DA, Lauterbur PC. Dendrimer-based metal chelates: A new class of magnetic resonance imaging contrast agents. Magn Reson Med 1994;31:1–8. [PubMed: 8121264]
25. Shukla R, Thomas TP, Peters J, Kotlyar A, Myc A, Baker JR Jr. Tumor angiogenic vasculature targeting with PAMAM dendrimer-RGD conjugates. Chem Commun(Camb) 2005;(46):5739–5741. [PubMed: 16307130]
26. Shukla R, Thomas TP, Peters JL, Desai AM, Kukowska-Latallo J, Patri AK, Kotlyar A, Baker JR Jr. HER2 specific tumor targeting with dendrimer conjugated anti-HER2 mAb. Bioconjug Chem 2006;17:1109–1115. [PubMed: 16984117]
27. Barth RF, Soloway AH, Adams DM, Alam F. Delivery of boron-10 for neutron capture therapy by means of monoclonal antibody-starburst dendrimer immunoconjugates. 1992
28. Malik N, Evagorou EG, Duncan R. Dendrimer-platinate: A novel approach to cancer chemotherapy. Anticancer Drugs 1999;10:767–776. [PubMed: 10573209]
29. Malik N, Wiwattanapatapee R, Klopsch R, Lorenz K, Frey H, Weener JW, Meijer EW, Paulus W, Duncan R. Dendrimers: Relationship between structure and biocompatibility in vitro, and preliminary studies on the biodistribution of 125I-labelled polyamidoamine dendrimers in vivo. J Control Release 2000;65:133–148. [PubMed: 10699277]
30. Mullen DG. Unpublished.
31. Choi Y, Thomas T, Kotlyar A, Islam MT, Baker JR Jr. Synthesis and functional evaluation of DNA-assembled polyamidoamine dendrimer clusters for cancer cell-specific targeting. Chem Biol 2005;12:35–43. [PubMed: 15664513]
32. Goyal P, Yoon K, Weck M. Multifunctionalization of dendrimers through orthogonal transformations. Chemistry 2007;13:8801–8810. [PubMed: 17508379]
33. Wu P, Malkoch M, Hunt JN, Vestberg R, Kaltgrad E, Finn MG, Fokin VV, Sharpless KB, Hawker CJ. Multivalent, bifunctional dendrimers prepared by click chemistry. Chem Commun(Camb) 2005;(46):5775–5777. [PubMed: 16307142]
34. Hill E, Shukla R, Park SS, Baker JR Jr. Synthetic PAMAM-RGD conjugates target and bind to odontoblast-like MDPC 23 cells and the predentin in tooth organ cultures. Bioconjug Chem 2007;18:1756–1762. [PubMed: 17970585]
35. Binder WH, Kluger C. Azide/alkyne-“click” reactions: Applications in material science and organic synthesis. Current Organic Chemistry 2006;10:1791.
36. Lee JW, Kim JH, Kim HJ, Han SC, Kim JH, Shin WS, Jin SH. Synthesis of symmetrical and unsymmetrical PAMAM dendrimers by fusion between azide- and alkyne-functionalized PAMAM dendrons. Bioconjug Chem 2007;18:579–584. [PubMed: 17335177]
37. Lee JW, Kim JH, Kim BK. Synthesis of azide-functionalized PAMAM dendrons at the focal point and their application for synthesis of PAMAM- like dendrimers. Tetrahedron Letters 2006;47:2683–2686.
38. Brooks PC, Clark RA, Cheresh DA. Requirement of vascular integrin alpha v beta 3 for angiogenesis. Science 1994;264:569–571. [PubMed: 7512751]
39. Cleaver O, Melton DA. Endothelial signaling during development. Nat Med 2003;9:661–668. [PubMed: 12778164]
40. Baillie CT, Winslet MC, Bradley NJ. Tumour vasculature--a potential therapeutic target. Br J Cancer 1995;72:257–267. [PubMed: 7543770]
41. Ruoslahti E. Specialization of tumour vasculature. Nat Rev Cancer 2002;2:83–90. [PubMed: 12635171]
42. Arap W, Pasqualini R, Ruoslahti E. Cancer treatment by targeted drug delivery to tumor vasculature in a mouse model. Science 1998;279:377–380. [PubMed: 9430587]
43. Los M, Voest EE. The potential role of antivascular therapy in the adjuvant and neoadjuvant treatment of cancer. Semin Oncol 2001;28:93–105. [PubMed: 11254869]

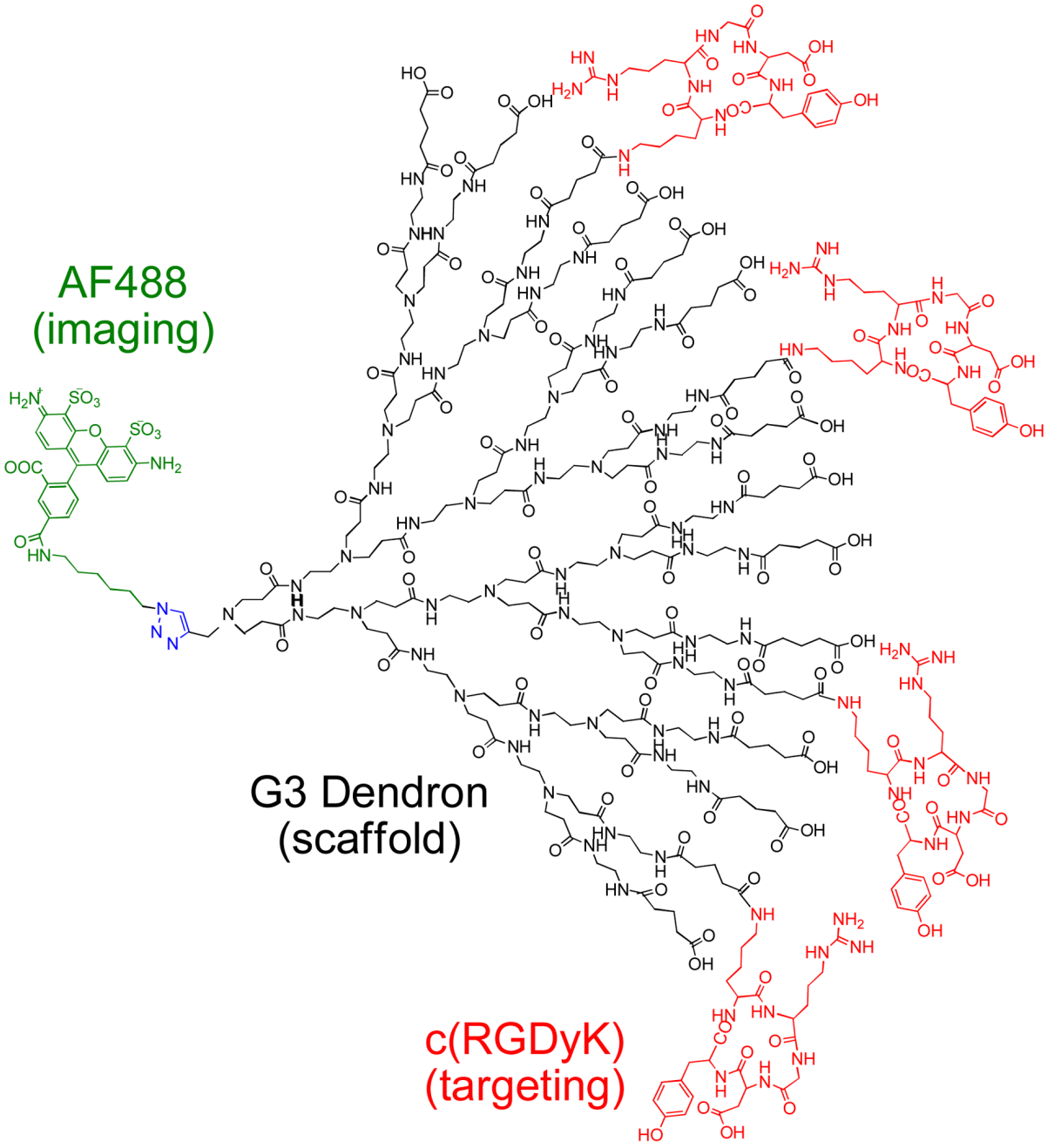

Figure 1.
Dendron conjugate AF-G3$(COOH)_{11.9}(RGD)_{4.1}$ **(4)** where Alexa Fluor 488 is conjugated to the dendron focal point via a 1,3-dipolar cycloaddition. The targeting moiety, c(RGDyK) peptide, is conjugated to the carboxylated surface of the dendron.

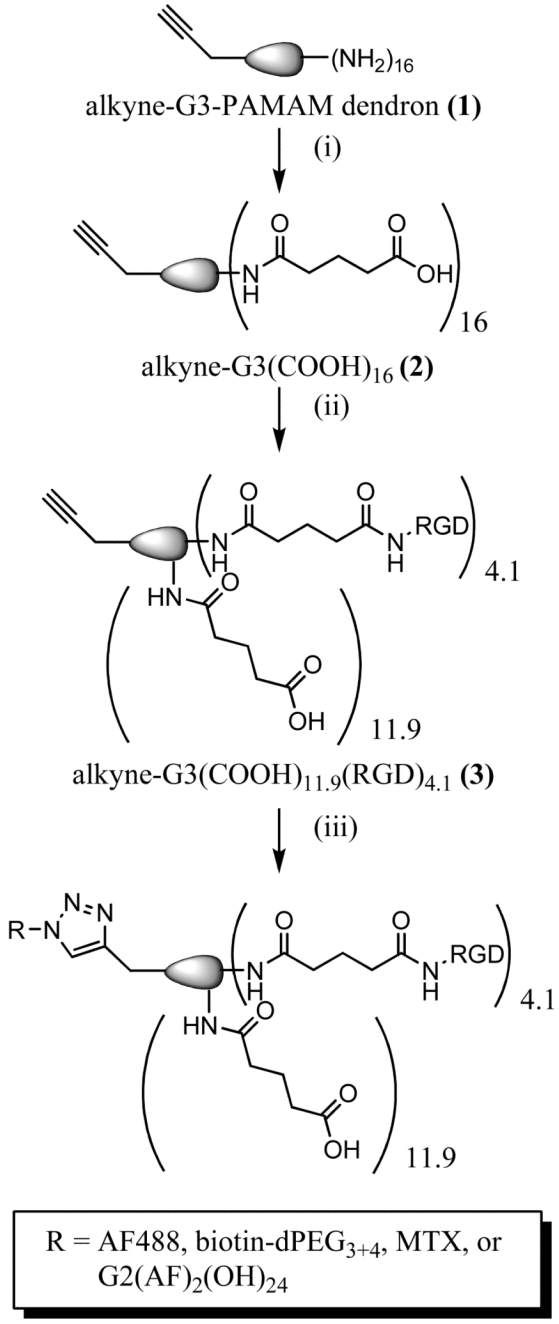

Figure 2.

Reaction scheme for creating click-conjugated dendrons employed in the *in vitro* studies. (i) glutaric anhydride, MeOH, 24 hrs, r.t. (ii) EDC, c(RGDyK), H_2O/DMSO, 2 days, r.t. (iii) Alexa Fluor 488 azide OR biotin-dPEG$_{3+4}$-azide OR MTX-azide**(5)** OP azide-G2(AF)$_2$(OH)$_{24}$ **(9)** sodium ascorbate, copper (II) sulfate, H_2O, 36 hours, r.t.

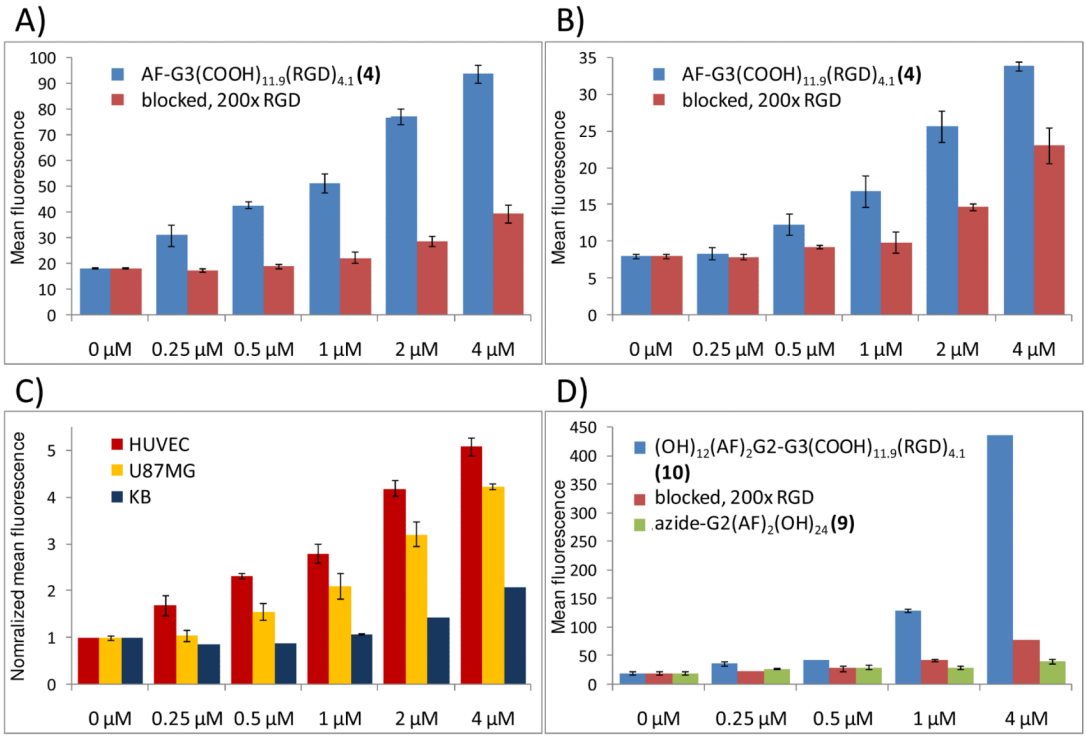

Figure 3.

Dose dependent uptake and specific targeting of binary dendrons determined via flow cytometry, with mean fluorescence plotted against the concentration of the dendron conjugate. Specific targeting of AF-G3(COOH)$_{11.9}$(RGD)$_{4.1}$ **(4)** was displayed in human umbilical vein endothelial cells (HUVEC) (A), and U87MG human glioblastoma cells (B). Blocking of **4** at all tested concentrations with a 200-fold molar excess of c(RGDyK) confirms specific targeting of the $\alpha_V\beta_3$ integrin by the dendron. A cell-line comparison between HUVEC, U87MG, and $\alpha_V\beta_3$ integrin deficient KB cells (C) shows dendron uptake is greater in cell lines with increased $\alpha v\beta_3$ integrin expression, demonstrating the active targeting capability of the binary dendron. A significant increase in mean fluorescence was displayed for a co-dendron structure capable of carrying additional dye, (OH)$_{24}$(AF)$_2$G2-G3(COOH)$_{11.9}$(RGD)$_{4.1}$ **(10)**, in HUVEC (D). The specific uptake of the co-dendron was confirmed by inhibition with free RGD as well as from a non-targeted control, azide-G2(AF)$_2$(OH)$_{24}$ **(9)**. Error bars indicate standard deviation as computed from the half-peak coefficient of variation.

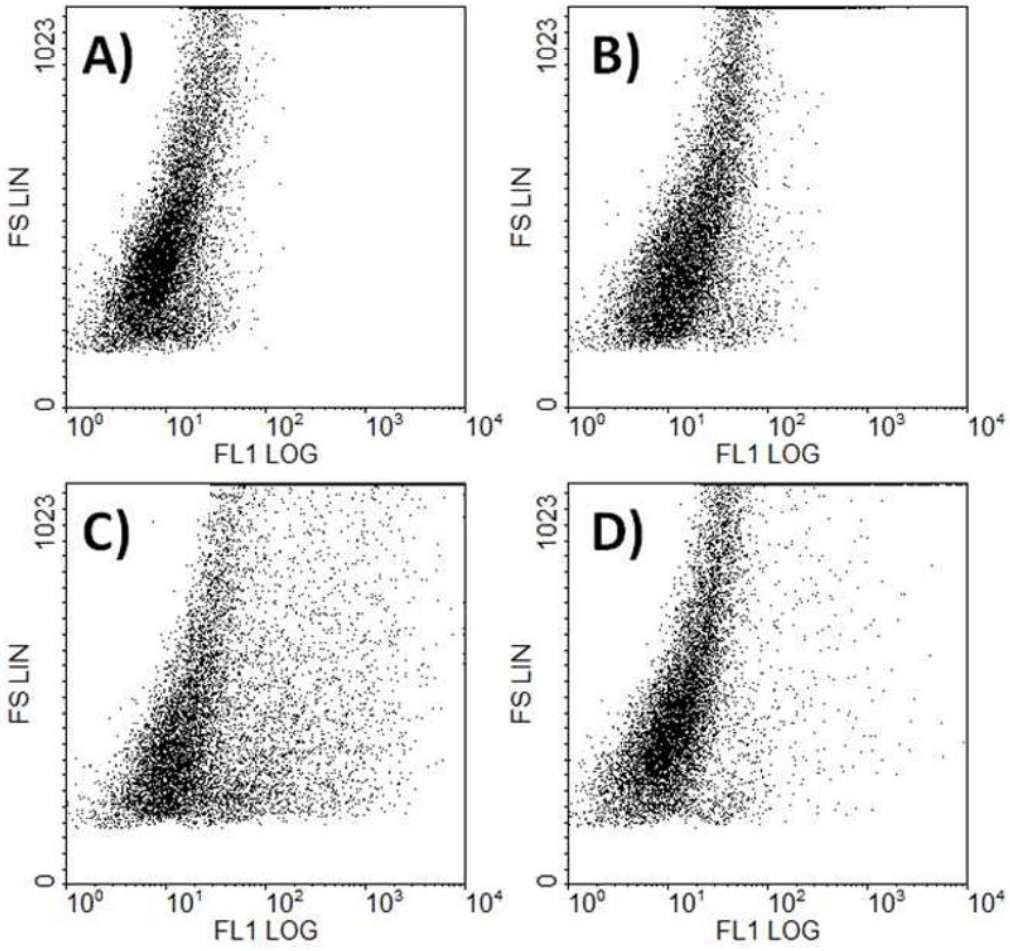

Figure 4.

Flow cytometry plot of fluorescence versus forward scatter for $(OH)_{24}(AF)_2G2$-$G3(COOH)_{11.9}(RGD)_{4.1}$ **(10)** at 4 μM. The co-dendron conjugate (C) shows a significant broading in cell population compared to the untreated control (A). When pre-incubated with a 200-fold molar excess of free RGD (D), **10** is partially blocked, but out-competes the excess monomeric RGD. The non-targeted control (B), azide-$G2(AF)_2(OH)_{24}$ **(9)**, shows no significant change in cell population when compared to the control.

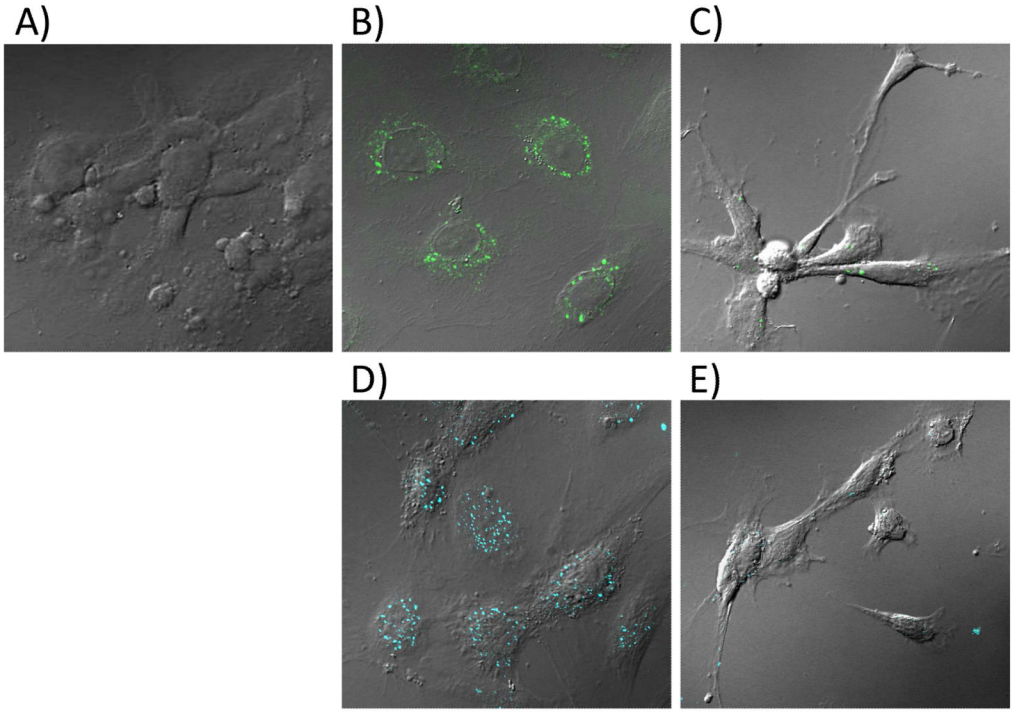

Figure 5.

Confocal images of HUVEC cells either untreated (A) or treated with 0.5 μM $(OH)_{24}(AF)_2G2\text{-}G3(COOH)_{11.9}(RGD)_{4.1}$ **(10)** (B–C) or biotin-$G3(COOH)_{11.9}(RGD)_{4.1}$ **(7)** (D–E) dendron for 2 hours. Samples C and E were pre-incubated with 100 μM c(RGDyK). Biotin-conjugated dendrons were detected by the addition of NeutrAvidin-Dylight 405.

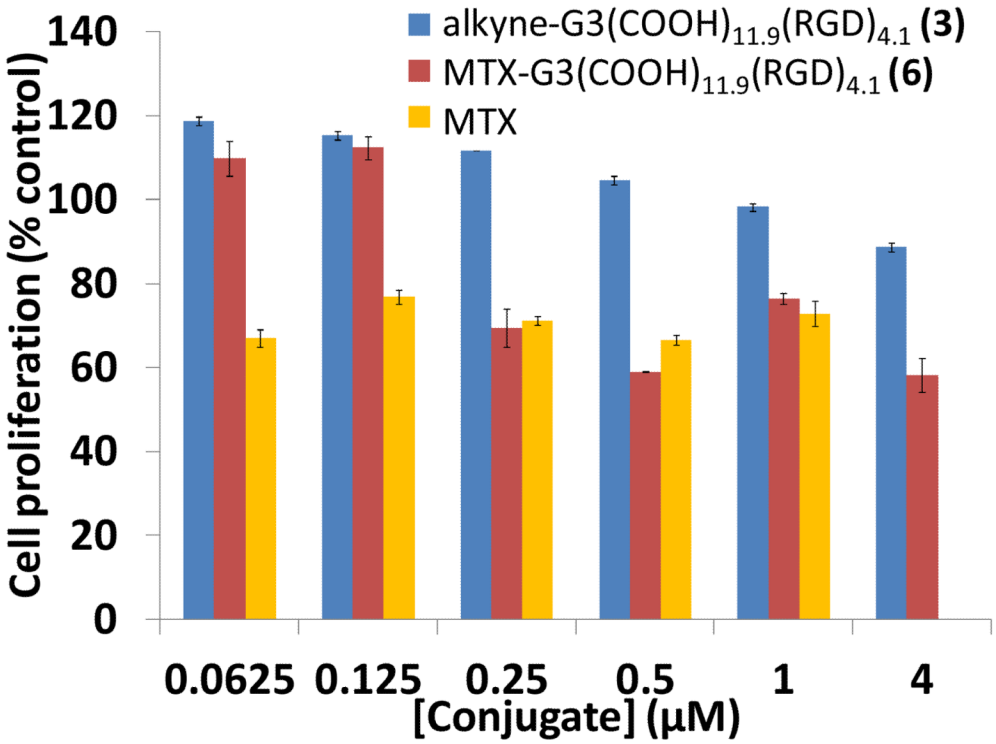

Figure 6.

The antiproliferative effect of MTX-G3$(COOH)_{11.9}(RGD)_{4.1}$ **(6)**. The dose-dependent inhibition of cell growth of **6** was compared to free MTX and alkyne-G3$(COOH)_{11.9}(RGD)_{4.1}$ control **(3)** using a XTT assay. The cells were treated with different concentrations of free MTX or dendron conjugates for 72 hours with a replenishing of 100 μL medium and the conjugates after 48 hours. **6** and MTX were determined to not be significantly different for concentrations greater than or equal to 0.25 μM. The effects of **6** and MTX were not significantly different for concentrations greater than 0.125 μM. **6** had a significantly greater effect on cell viability versus **3** for concentrations greater than 0.125 μM.